length of the bonding wires which at this frequency have an inductive reactance of approximately 6 Ω/0.001 in of length. Future efforts on this mixer will be concentrated on keeping these wires as short and as equal as possible.

These experiments have confirmed the theoretical predictions of Section II and demonstrated the usefulness of the antiparallel diode pair as a harmonic mixer. Potentially the most useful application of this circuit will be at millimeter wavelengths although careful balancing of the diodes will be required to realize its full potential.

REFERENCES

[1] M. Cohn, F. L. Wentworth, and J. C. Wiltse, "High-sensitivity 100- to 300-Gc radiometers," *Proc. IEEE*, vol. 51, pp. 1227–1232, Sept. 1963.
[2] R. J. Bauer, M. Cohn, J. M. Cotton, Jr., and R. F. Packard, "Millimeter wave semiconductor diode detectors, mixers, and frequency multipliers," *Proc. IEEE (Special Issue on Millimeter Waves and Beyond)*, vol. 54, pp. 595–605, Apr. 1966.
[3] R. Meredith and F. L. Warner, "Superheterodyne radiometers for use at 70 Gc and 140 Gc," *IEEE Trans. Microwave Theory Tech.*, vol. MTT-11, pp. 397–411, Sept. 1963.
[4] F. A. Benson, *Millimetre and Submillimetre Waves*. London, England: Iliffe Books, 1969, ch. 22.
[5] M. Cohn, J. E. Degenford, and B. A. Newman, "Harmonic mixing with an anti-parallel diode pair," in *1974 MTT Int. Symp. Dig.*, pp. 171–172, June 12–14, 1974.
[6] M. R. Barber, "Noise figure and conversion loss of the Schottky barrier mixer diode," *IEEE Trans. Microwave Theory Tech.*, vol. MTT-15, pp. 629–635, Nov. 1969.
[7] M. V. Schneider, "Harmonically pumped stripline down converter," presented at the European Microwave Conf., Montreux, Switzerland, Sept. 10–13, 1974.
[8] J. B. Cahalan, J. E. Degenford, and M. Cohn, "An integrated X-band, image and sum frequency enhanced mixer with 1 GHz IF," in *1971 IEEE Int. Microwave Symp. Dig.* (Washington, D. C.), May 17–19, 1971.

Effect of Temperature on Device Admittance of GaAs and Si IMPATT Diodes

YOICHIRO TAKAYAMA, MEMBER, IEEE

Abstract—**The effect of temperature on the small-signal admittance of IMPATT diodes with uniformly doped and high–low doped (Read) structures is investigated experimentally and theoretically. Small-signal admittance characteristics of X-band Si p^+-n-n^+, GaAs M-n-n^+ (Schottky-uniform), and GaAs M-n^+-n-n^+ (Schottky–Read) IMPATT diodes are measured at various junction temperatures for different dc current levels. Small-signal analysis is performed on GaAs IMPATT diodes of uniformly doped and high–low doped structures, and the calculated results on temperature dependence of the device admittance are compared with the experimental results. Reasonable agreement is found between theory and experiment. It is shown that GaAs IMPATT diodes are superior to Si diodes in admittance temperature characteristics and that the uniformly doped structure has a small admittance temperature coefficient in magnitude, compared to the high–low doped structure. It is also shown by calculation that the admittance temperature coefficient of a punch-through diode is small in magnitude, compared to that of a non-punch-through diode.**

I. INTRODUCTION

RECENTLY, Si and GaAs IMPATT diodes with various structures have been developed. In their applications to microwave oscillators and amplifiers, temperature variation of operating characteristics, such as frequency, power, phase, and noise, is a serious problem. The temperature dependence of the device admittance of IMPATT diodes is a fundamental factor for assessing the temperature characteristics of IMPATT oscillators and amplifiers. Temperature dependence of small-signal admittance of IMPATT diodes has been calculated by several authors for restricted structures and operating conditions [1]–[4]. However, those previous works are fragmental and do not present a sufficiently detailed picture. Furthermore, no experimental investigation to determine temperature effect on IMPATT diode admittance has been reported so far.

The purpose of this paper is to present a basic understanding of temperature effect on small-signal admittance of IMPATT diodes with various structures, and to provide an available guide for network and device design, considering the temperature effect. Small-signal admittance characteristics of X-band Si p^+-n-n^+, GaAs M-n-n^+ (Schottky, uniformly doped), and GaAs M-n^+-n-n^+ (Schottky–Read) IMPATT diodes were measured at various junction temperatures for different dc current levels. Small-signal analyses of GaAs IMPATT diodes with the uniformly doped and high–low doped (or Read-type) structures were performed and the calculated results on the temperature characteristics of GaAs IMPATT diode admittance are compared to the experiments. Reasonable agreement was found in the temperature dependence of the device admittance between theoretical and experimental results.

Manuscript received August 22, 1974; revised March 20, 1975.
The author is with Central Research Laboratories, Nippon Electric Company, Nakahara-ku, Kawasaki, Japan.

II. CHARACTERIZATION OF IMPATT DIODES

In this section, first, a method of characterizing IMPATT diodes is described and, then, the experimental results showing the temperature effect on the small-signal admittance of Si p^+-n-n^+, GaAs M-n-n^+ (Schottky-uniform), and GaAs M-n^+-n-n^+ (Schottky–Read) IMPATT diodes are presented.

A block diagram of the circuit used for diode admittance measurement is shown in Fig. 1. The transforming network includes package parasitics and diode-mounting circuit and is assumed to be lossy and linear. Diode admittance Z_d is obtained through bilinear transformations, which are determined by the least square method for low frequency and microwave measurements at several prebreakdown bias voltages [5].

The equivalent circuit of the IMPATT diode at prebreakdown bias condition is shown in Fig. 2, where $C_j(V)$ represents the voltage-dependent junction capacitance, and R_s is the diode series resistance [6], which consists of the resistance of the undepleted region, and spreading and contact resistances. Voltage-dependent resistance $R_u(V)$ is defined to be zero at the breakdown voltage. In the data processing, voltage-independent resistance R_{s0} is assigned to the transforming network. The resistance $R_u(V)$ is large in Read diodes [7], while, in the GaAs uniformly doped diode, R_u is negligibly small for determining the bilinear transformations. The series resistance of the undepleted region is calculated by integration of the carrier concentration multiplied by the carrier mobility. The doping profiles are calculated from the capacitance–voltage data measured at 1 MHz.

Junction capacitance C_j and series resistance R_u of the X-band GaAs high–low doped diode (Schottky–Read type), as functions of reverse bias voltage before breakdown, are shown in Fig. 3. The doping profile is also shown in the figure. R_u is relatively large in the Read diode because of the high resistivity of the low-doped region.

A. Data Processing

In the measurement system shown in Fig. 1, diode impedance Z_d is transformed into an input reflection coefficient Γ_{in} through the transforming network. Assuming the linear transforming network, the functional dependence between Γ_{in} and Z_d has the form of a bilinear transformation

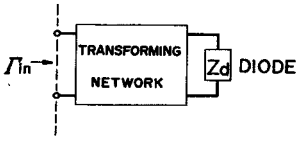

Fig. 1. Block diagram of IMPATT diode measurement circuit.

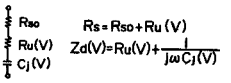

Fig. 2. Equivalent circuit of IMPATT diode before breakdown.

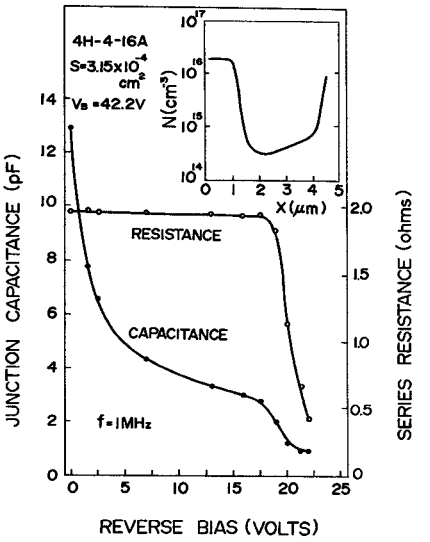

Fig. 3. Junction capacitance and series resistance of X-band GaAs high–low doped diode (Schottky–Read type) as a function of reverse bias voltage before breakdown, and doping profile.

$$\Gamma_{in} = \frac{KZ_d + L}{MZ_d + 1} \tag{1}$$

where bilinear transformation cofficients K, L, and M are complex constants. The numerical data processing, necessary to determine coefficients K, L, and M, is based on an extension of Kajfez's least square method [5], [7]. In contrast with Kajfez's case for the varactor diode, Z_d before breakdown is complex as

$$Z_d(V) = R_u(V) + \frac{1}{j\omega C_j(V)}. \tag{2}$$

For a number $N(N \geq 3)$ of pairs of measured points Γ_n and Z_n, in a similar way to Kajfez's discussion, we obtain the following system of six equations

$$\begin{aligned}
&K_r\Sigma(Z_r^2 + Z_i^2) + L_r\Sigma Z_r + L_i\Sigma Z_i - M_r\Sigma(Z_r^2 + Z_i^2)\Gamma_r \\
&\qquad + M_i\Sigma(Z_r^2 + Z_i^2)\Gamma_i = \Sigma(Z_r\Gamma_r + Z_i\Gamma_i) \\
&K_i\Sigma(Z_r^2 + Z_i^2) - L_r\Sigma Z_i + L_i\Sigma Z_r - M_r\Sigma(Z_r^2 + Z_i^2)\Gamma_i \\
&\qquad - M_i\Sigma(Z_r^2 + Z_i^2)\Gamma_r = \Sigma(Z_r\Gamma_i - Z_i\Gamma_r) \\
&K_r\Sigma Z_r - K_i\Sigma Z_i + L_rN - M_r\Sigma(Z_r\Gamma_r - Z_i\Gamma_i) \\
&\qquad + M_i\Sigma(Z_i\Gamma_r + Z_r\Gamma_i) = \Sigma\Gamma_r \\
&K_r\Sigma Z_i + K_i\Sigma Z_r + L_iN - M_r\Sigma(Z_i\Gamma_r + Z_r\Gamma_i) \\
&\qquad - M_i\Sigma(Z_r\Gamma_r - Z_i\Gamma_i) = \Sigma\Gamma_i \\
&K_r\Sigma(Z_r^2 + Z_i^2)\Gamma_r + K_i\Sigma(Z_r^2 + Z_i^2)\Gamma_i \\
&\quad + L_r\Sigma(Z_r\Gamma_r - Z_i\Gamma_i) + L_i\Sigma(Z_i\Gamma_r + Z_r\Gamma_i) \\
&\quad - M_r\Sigma(Z_r^2 + Z_i^2)(\Gamma_r^2 + \Gamma_i^2) = \Sigma(\Gamma_r^2 + \Gamma_i^2)Z_r \\
&K_r\Sigma(Z_r^2 + Z_i^2)\Gamma_i - K_i\Sigma(Z_r^2 + Z_i^2)\Gamma_r \\
&\quad + L_r\Sigma(Z_i\Gamma_r + Z_r\Gamma_i) - L_i\Sigma(Z_r\Gamma_r - Z_i\Gamma_i) \\
&\quad + M_i\Sigma(Z_r^2 + Z_i^2)(\Gamma_r^2 + \Gamma_i^2) = \Sigma(\Gamma_r^2 + \Gamma_i^2)Z_i.
\end{aligned} \tag{3}$$

For simplicity of writing, the subscripts n have been omitted from the above expressions. Subscripts r and i denote real and imaginary parts, respectively. This system of six equations can be solved by the use of a digital computer.

The obtained bilinear transformation coefficients are used to deduce the diode active impedance from the microwave data measured at bias points beyond breakdown, as

$$Z_d = \frac{L - \Gamma_{in}}{M\Gamma_{in} - K}. \quad (4)$$

B. Experimental

X-band Si p^+-n-n^+, GaAs M-n-n^+ (Pt Schottky barrier, uniformly doped), and GaAs M-n^+-n-n^+ (Pt Schottky barrier, high–low doped Read) diodes [8] have been investigated. Some physical parameters of the diodes are listed in Table I. The uniformly doped diodes are not punched through at breakdown and the high–low doped diodes are punched through. The microwave measurement was made using a 50-Ω coaxial test mount, as shown in Fig. 4. The mount is made of super Invar. Temperature control was carried out by means of a thermopanel. The method of junction temperature evaluation is described in the next subsection. The reflection coefficient was measured with a network analyzer reflection test system.

Measured small-signal admittance characteristics are shown in Figs. 5, 6, and 7, with dc current and frequency as parameters. It is seen that the Read diode has a rela-

TABLE I
PHYSICAL PARAMETERS OF IMPATT DIODES USED IN EXPERIMENTS

	Si p^+-n-n^+	GaAs M-n-n^+	GaAs M-n^+-n-n^+	
	10x-8	EGM39-9	4H-4-16A-1	4H-4-16A-12
$S(cm^2)$	2.6×10^{-4}	3.7×10^{-4}	3.15×10^{-4}	3.58×10^{-4}
C_{jB}(pF)	0.73	0.60	0.67	0.78
$n(cm^{-3})$	7×10^{15}	1.2×10^{16}	see Fig.3	
$W_B(\mu m)$	2.7	2.5	4.3	4.4
V_B(V)	69.0	54.6	42.2	46.3
V_D(V)	84.5	69.7	—	71.5

S : junction area, C_{jB} : junction capacitance at breakdown, n : doping level, W_B : depletion region width at breakdown, V_B : breakdown voltage, V_D : dc voltage for dc current I_o = 140mA at junction temperature T_j = 200°C

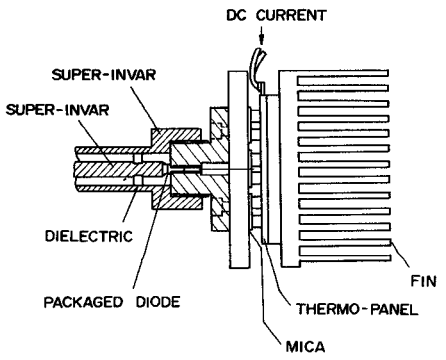

Fig. 4. Coaxial test mount for microwave measurements.

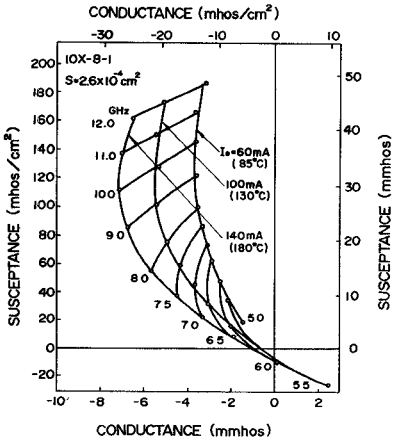

Fig. 5. Measured small-signal admittance of Si p^+-n-n^+ IMPATT diode with dc current and frequency as parameters.

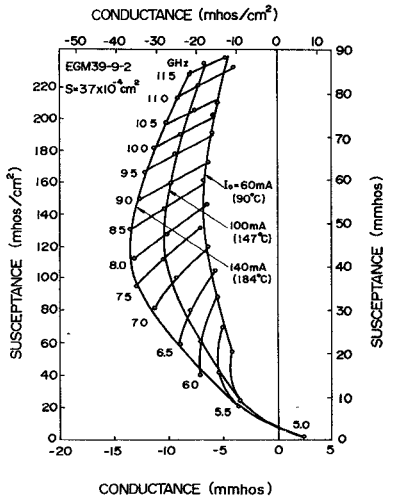

Fig. 6. Measured small-signal admittance of GaAs M-n-n^+ IMPATT diode with dc current and frequency as parameters.

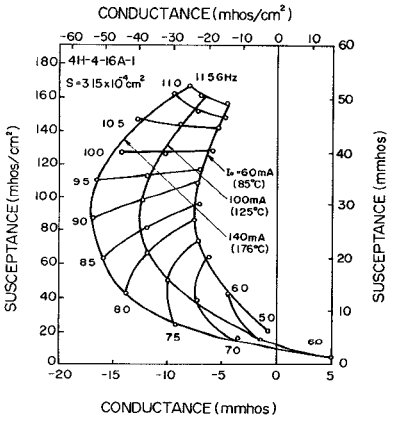

Fig. 7. Measured small-signal admittance of GaAs Schottky–Read diode with dc current and frequency as parameters.

tively narrow peak negative conductance versus frequency and a relatively low negative Q (ratio of conductance to susceptance), while the uniformly doped diodes exhibit a wider frequency range with some reduction of peak conductance value. In addition, GaAs IMPATT diodes have larger negative conductance and lower negative Q, compared to Si diodes.

C. Temperature Characteristics

Small-signal admittance measurements at various junction temperatures were made for different dc current levels on the three types of diodes. Diode junction temperature was controlled with the thermopanel. The temperature was monitored by dc terminal voltage V_D which had been determined, in advance, as a function of junction temperature T_j for a given dc current I_0, as

$$V_D(T_j) = V_B(T_j) + R_{SC}(T_j,I_0)I_0 \qquad (5)$$

where V_B is the temperature dependent breakdown voltage and R_{SC} is the space-charge resistance. R_{SC} was measured at 5 MHz [9].

In the admittance measurement, the junction temperature was set at several points between 60°C and 240°C. The small-signal conductances and susceptances of Si p^+-n-n^+, GaAs M-n-n^+, and GaAs M-n^+-n-n^+ (Schottky–Read) diodes for I_0 = 140 mA at several junction temperatures are shown in Figs. 8, 9, and 10, respectively. The temperature dependence of the diode admittance is characterized by temperature coefficients θ_G and θ_B, defined as

$$\theta_G = \frac{1}{G_d}\cdot\frac{\Delta G_d}{\Delta T_j}, \qquad \theta_B = \frac{1}{B_d}\cdot\frac{\Delta B_d}{\Delta T_j} \qquad (6)$$

where

$$\Delta G_d = G_d(T_2) - G_d(T_1)$$
$$\Delta B_d = B_d(T_2) - B_d(T_1)$$
$$\Delta T_j = T_2 - T_1.$$

The temperature coefficients obtained experimentally for Si p^+-n, GaAs M-n, and GaAs M-n^+-n diodes are shown in Figs. 11, 12, and 13, respectively. Measurements were made at dc current levels of I_0 = 60, 100, and

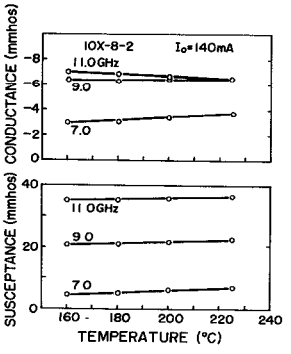

Fig. 8. Measured small-signal conductance and susceptance of Si p^+-n-n^+ IMPATT diode for I_0 = 140 mA as a function of junction temperature.

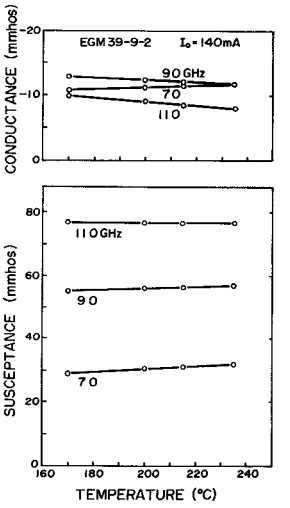

Fig. 9. Measured small-signal conductance and susceptance of GaAs M-n-n^+ IMPATT diode for I_0 = 140 mA as a function of junction temperature.

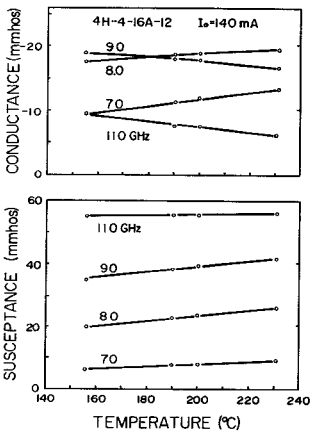

Fig. 10. Measured small-signal conductance and susceptance of GaAs M-n^+-n-n^+ (Schottky–Read) diode for I_0 = 140 mA as a function of junction temperature.

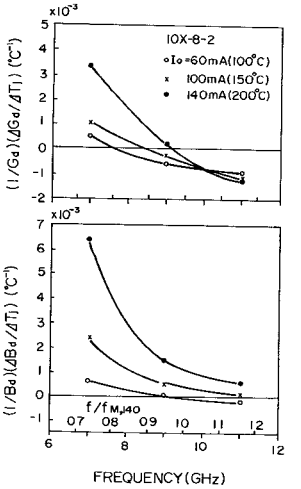

Fig. 11. Measured admittance temperature coefficients of Si p^+-n-n^+ IMPATT diode for dc current levels of 60, 100, and 140 mA.

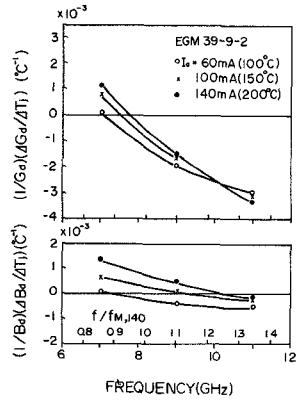

Fig. 12. Measured admittance temperature coefficients of GaAs M-n-n$^+$ IMPATT diode for dc current levels of 60, 100, and 140 mA.

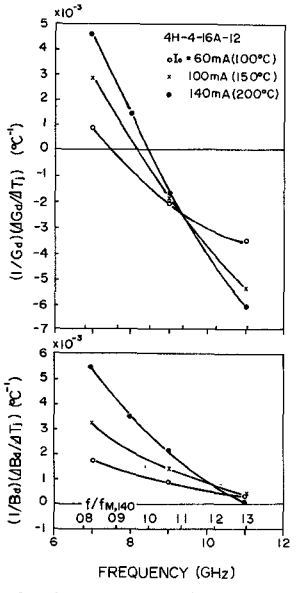

Fig. 13. Measured admittance temperature coefficients of GaAs Schottky–Read diode for dc current levels of 60, 100, and 140 mA.

140 mA. The coefficients were obtained at $T_j = 100$°C for $I_0 = 60$ mA, $T_j = 150$°C for $I_0 = 100$ mA, and $T_j = 200$°C for $I_0 = 140$ mA, setting $\Delta T_j \sim 50$°C. In the figures, f_M is the peak frequency where the peak negative conductance is obtained for $I_0 = 140$ mA.

D. Discussion

In all these diodes, the conductance temperature coefficients at a given dc current are positive at lower frequencies, decrease with an increase of frequency, and become negative at higher frequencies. The susceptance temperature coefficients are positive for the most part of the frequency range, decrease with an increase of frequency, and get nearer to zero or become negative, in some cases, at higher frequencies. With an increase of dc current, the temperature coefficients enlarge in magnitude in the main frequency range.

In regard to the uniformly doped structures, the experimental result shows the superiority of the GaAs diode to the Si diode in the admittance temperature characteristics from the viewpoint of frequency variation of the oscillators. It is also seen that the GaAs high–low doped or Read diode is inferior to the GaAs uniformly doped diode in admittance temperature characteristics. The GaAs Read diode is also inferior to the Si uniformly doped diode. The inferiority of the Read diode, especially in its conductance temperature characteristics, seems to be associated with its relatively high and narrow peak negative conductance. These experimental results show reasonable agreement with the calculated results which will be described in the next section.

It should be noted that the active depletion region in the non-punch-through diode extends with an increase of junction temperature and of space charge-density or of dc current. The expansion of the depletion region width results in an increase of the series resistance R_u, and this produces an error in the data-processed results. This error may pose a slight problem in the Si p$^+$-n diode which has a somewhat larger resistance R_u, compared to that of the GaAs M-n diode. However, in the above mentioned case, deviation of the admittance is less than 1 percent in magnitude, and variation of the undepleted resistance with temperature is about 5×10^{-4} Ω/°C or less, which is not much variation. Therefore, the depletion region extension was neglected, though it can be compensated for, if necessary.

III. ANALYSES

Small-signal analyses of GaAs IMPATT diodes with uniformly doped and high–low doped structures were performed, based on the model described by Gilden and Hines [10].

The high–low doped structure is shown in Fig. 14(a), where x_0 is the width of the high-doped (n_1) region, W the total depletion width, and L the sum of the width of the high-doped and low-doped (n_2) region. The n^+ region is the very heavily doped substrate. Fig. 14(b) shows the electric field distribution for the high–low doped structure.

Small-signal analyses were performed for GaAs diodes using an equal ionization rate for electrons and holes given [11] by

$$\alpha = \alpha_\infty \exp\{-(b/E)^2\} \tag{7}$$

where E is the electric field and

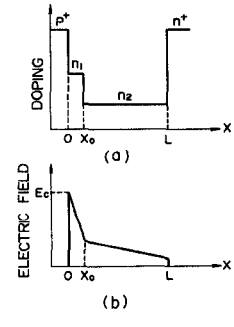

Fig. 14. High–low doped structure considered in the text. (a) Doping profile. (b) Electric-field profile.

$$\alpha_\infty = 2.0 \times 10^5 + 140.0 \times (T_j - 25.0) \text{ cm}^{-1} \quad (8)$$

$$b = 5.5 \times 10^5 + 660.0 \times (T_j - 25.0) \text{ V/cm}. \quad (9)$$

α_∞ is assumed to increase linearly with an increase of temperature, at a rate of 7 percent/100°C, and so does b, at a rate of 12 percent/100°C [11]. The velocity of electrons and of holes are assumed to be equal and saturated in the depletion region, and is expressed as

$$V_{s1} = 8 \times 10^6 - 1.14 \times 10^4 \times (T_j - 25.0) \text{ cm/s}. \quad (10)$$

It gives 8×10^6 cm/s at $T_j = 25$°C and 6×10^6 cm/s at $T_j = 200$°C [2], and is assumed to decrease linearly with an increase of temperature.

The small-signal impedance Z given by Gilden and Hines [10] is

$$Z = \frac{V_{s1}}{A\epsilon_s\omega^2} \cdot \frac{1}{1 - \omega^2/\omega_r^2} \cdot (1 - \cos\theta_d) + R_s + j\frac{1}{\omega C_d}\left[\left(\frac{\sin\theta_d}{\theta_d} - 1\right) - \left(\frac{\sin\theta_d/\theta_d + X_A/(W - X_A)}{1 - \omega_r^2/\omega^2}\right)\right] \quad (11)$$

where X_A is the avalanche region width, ϵ_s the dielectric permitivity ($\epsilon_s/\epsilon_0 = 10.9$), A the junction area, ω_r the avalanche frequency, R_S the passive resistance of the undepleted region, and

$$\theta_d = \frac{\omega(W - X_A)}{V_{s1}}$$

$$C_d = \frac{A\epsilon_s}{W - X_A}.$$

The avalanche frequency ω_r is given as

$$\omega_r = \left(\frac{2\alpha' V_{s1} J_0}{\epsilon_s}\right)^{1/2}$$

where J_0 is the dc current density and $\alpha' = d\alpha/dE$ at the maximum field Ec. Note that α' is temperature dependent. R_S is given by

$$R_s = \frac{L - W}{en\mu A}$$

where μ is the low-field carrier mobility and n the carrier density in the undepleted region.

The critical field E_c is obtained from the avalanche breakdown condition

$$\int_0^W \alpha(E)\, dx = 1 \quad (12)$$

and the avalanche width X_A is defined [12] as the distance over which 95 percent of the contribution to the integral is obtained, i.e.,

$$\int_0^{X_A} \alpha(E)\, dx = 0.95. \quad (13)$$

The electric-field distribution in the high–low doped structure is given by

$$E_1(x) = E_c - \frac{e(n_1 - n_s)}{\epsilon_s} x, \qquad 0 \le x \le x_0$$

$$E_2(x) = E_c - \frac{e(n_1 - n_2)}{\epsilon_s} x_0 - \frac{e(n_2 - n_s)}{\epsilon_s} x, \qquad x_0 \le x \le L$$

$$E_3(x) = E_c - \frac{e(n_1 - n_2)}{\epsilon_s} x_0 - \frac{e(n_2 - n^+)}{\epsilon_s} L - \frac{en^+}{\epsilon_s} x, \qquad L < x \quad (14)$$

where the space charge due to the dc current is assumed to be uniform as

$$n_s = \frac{J_0}{eV_{s1}}. \quad (15)$$

A. Diode Samples

The three types of GaAs IMPATT diodes listed in Table II were investigated, which correspond to the samples used in the experiments. Sample M-N1-1 is a non-punch-through diode with uniformly doped structure. Sample M-N1-2 is a punch-through diode with uniformly doped structure. Sample M-N1-N2-1 is a high–low doped punch-through diode. A specific set of calculated results is also presented in Table II. The efficiency is very approximately given [13] by

$$\eta = \frac{1}{\pi} \cdot \frac{V_D - V_A}{V_D}$$

where V_D is the voltage drop across the active region, and V_A is the voltage drop across the avalanche region. The value of W in sample M-N1-2 is the extrapolated value of

TABLE II
GaAs IMPATT Diode Parameters Considered in Analyses

	Uniformly doped				High-low doped	
	M-N1-1		M-N1-2		M-N1-N2-1	
Doping (cm^{-3})	1.0×10^{16}		1.0×10^{16}		$n_1=2.0\times10^{16}$, $n_2=4.0\times10^{14}$	
L(μm)	3.0		2.4		4.2	
x_o(μm)	—		—		1.2	
J_o(A/cm^2)	200	400	200	400	200	400
T_j(°C)	150	200	150	200	150	200
W(μm)	2.65	2.81	2.65	2.81	—	—
x_A(μm)	0.772	0.806	0.772	0.806	0.479	0.496
V_D(V)	57.1	62.7	56.6	61.3	59.2	69.7
η(%)	16.0	16.2	15.8	15.8	21.4	22.4
f_M(GHz)	9.2	10.2	10.0	11.2	7.2	8.2
G_M ($mhos/cm^2$)	-17.7	-29.8	-16.9	-27.9	-25.2	-43.2

the distance where $E = 0$. f_M is the frequency at which the peak negative conductance G_M is obtained.

B. Results and Discussion

Conductance and susceptance temperature coefficients were calculated as

$$\theta_G = \frac{1}{G_d(T_j)} \cdot \frac{G_d(T_j + \Delta T) - G_d(T_j - \Delta T)}{2\Delta T} \quad (16)$$

$$\theta_B = \frac{1}{B_d(T_j)} \cdot \frac{B_d(T_j + \Delta T) - B_d(T_j - \Delta T)}{2\Delta T} \quad (17)$$

where $\Delta T = 25°C$ was adopted in the calculation. Calculated results, showing conductance and susceptance temperature coefficients of GaAs IMPATT diodes, are presented in Figs. 15, 16, and 17. Fig. 15 shows the admittance temperature coefficients of the non-punch-through diode with uniformly doped structure for dc current density $J_0 = 200$ A/cm² at junction temperature $T_j = 150°C$ and for $J_0 = 400$ A/cm² at $T_j = 200°C$. Fig. 16 shows the temperature coefficients of the punch-through diode with uniformly doped structure, and Fig. 17 shows the temperature coefficients of the Read diode with the high–low doped structure. In the figures, normalized frequency f/f_M for $J_0 = 400$ A/cm² is scaled in order to conveniently compare the values with the experimental results.

Comparing the analytical results with the experimental results, showing the temperature coefficients of the small-signal admittance of GaAs IMPATT diodes of uniformly doped and high–low doped structures, it is seen that both results are in fairly good agreement, not only qualitatively, but also quantitatively. At a given dc current, the conductance temperature coefficients are positive at lower frequencies, decrease with an increase of frequency, becoming negative at higher frequencies. The susceptance temperature coefficients are positive for the most part, decrease with an increase of frequency, getting nearer to zero or becoming negative in some cases at higher frequencies. Regardless of structures, the temperature coefficients enlarge in magnitude with an increase of dc current.

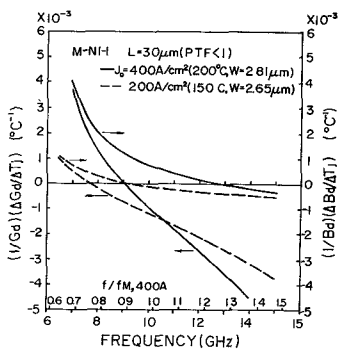

Fig. 15. Calculated admittance temperature coefficients of non-punch-through diode with GaAs uniformly doped structure for dc current densities of 200 and 400 A/cm².

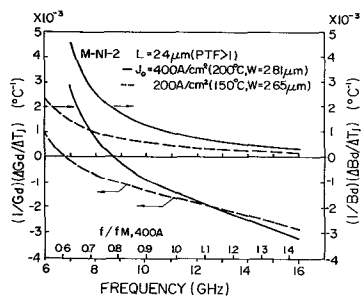

Fig. 16. Calculated admittance temperature coefficients of punch-through diode with GaAs uniformly doped structure for dc current densities of 200 and 400 A/cm².

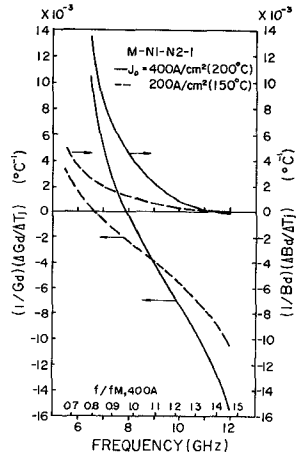

Fig. 17. Calculated admittance temperature coefficients of Read diode with GaAs high–low doped structure for dc current densities of 200 and 400 A/cm².

With regard to the effect of structures, it is seen that the high–low doped (or Read) structure has considerably larger admittance temperature coefficient in magnitude, compared with the uniformly doped structure. In general, it seems that a diode which is more like an ideal Read structure is more sensitive to the variation of material parameters and operating conditions. It is seen from Figs. 15 and 16 that the punch-through diode is superior to the non-punch-through diode in device admittance temperature characteristics.

IV. CONCLUSION

Temperature effect on small-signal admittance of IMPATT diodes with the uniformly doped and high–low doped Read structures has been investigated experimentally and theoretically. Small-signal admittance measurements were made at various junction temperatures for different dc current levels on X-band Si p^+-n-n^+, GaAs M-n-n^+, and GaAs M-n^+-n-n^+ (high–low Schottky–Read) IMPATT diodes. Small-signal analyses of GaAs IMPATT diodes were performed for uniformly doped and high–low doped structures. The calculated temperature dependence of device admittance were shown to be in reasonable agreement with the experimental results.

It was shown that GaAs IMPATT diodes are superior to Si diodes in device admittance temperature characteristics from the viewpoint of frequency variation of the oscillators and that the uniformly doped structure has superior admittance temperature characteristics, compared to the high–low doped structure. It was also shown theoretically that the admittance temperature coefficients of the punch-

through diode are small in magnitude, compared to the non-punch-through diode.

ACKNOWLEDGMENT

The author would like to thank F. Hasegawa and Y. Aono for providing the GaAs diodes and their helpful discussions, and H. Nagao in Semiconductor Division for supplying the Si diode pellets. He would also like to thank K. Ayaki, K. Sekido, and S. Nagano for their encouragement and guidance.

REFERENCES

[1] W. E. Schroeder and G. I. Haddad, "The effect of temperature on the operation of an IMPATT diode," *Proc. IEEE* (Lett.), vol. 59, pp. 1242–1244, Aug. 1971.
[2] ——, "Nonlinear properties of IMPATT devices," *Proc. IEEE*, vol. 61, pp. 153–182, Feb. 1973.
[3] T. Watanabe, M. Nakamura, K. Saito, and H. Kodera, "Temperature dependence of oscillation characteristics of GaAs Schottky barrier IMPATT diode," in *Rec. Professional Group on Electron Devices Inst. Electron. Commun. Eng.* (Japan), Feb. 1972, Paper ED71-62.
[4] J. R. Grierson, "Theoretical calculations on the effect of temperature on the operation of an IMPATT diode," *Electron. Lett.*, vol. 8, pp. 258–260, May 1972.
[5] D. Kajfez, "Numerical data processing of reflection coefficient circles," *IEEE Trans. Microwave Theory Tech.*, vol. MTT-18, pp. 96–100, Feb. 1970.
[6] J. W. Gewartowski and J. E. Morris, "Active IMPATT diode parameters obtained by computer reduction of experimental data," *IEEE Trans. Microwave Theory Tech.*, vol. MTT-18, pp. 157–161, Mar. 1970.
[7] Y. Takayama, "Comparative studies of GaAs Read, GaAs M-n and Si p^+-n IMPATT diodes with experimental characterization," in *Rec. Professional Group on Electron Devices Inst. Electron. Commun. Eng.* (Japan), Jan. 1974, Paper ED73-70.
[8] F. Hasegawa, Y. Aono, Y. Kaneko, and K. Sekido, "Experimental study of high-power GaAs Read-type IMPATT diode," in *Rec. Professional Group on Electron Devices Inst. Electron. Commun. Eng.* (Japan), Jan. 1974, Paper ED73-68.
[9] R. H. Haitz, H. L. Stover, and N. J. Tolar, "A method for heat flow resistance measurements in avalanche diodes," *IEEE Trans. Electron Devices*, vol. ED-16, pp. 438–444, May 1969.
[10] M. Gilden and M. E. Hines, "Electronic tuning effects in the Read microwave avalanche diode," *IEEE Trans. Electron Devices* (*Special Issue on Semiconductor Bulk-Effect and Transit-Time Devices*), vol. ED-13, pp. 169–175, Jan. 1966.
[11] R. Hall and J. H. Leck, "Temperature dependence of avalanche breakdown in gallium arsenide p-n junctions," *Int. J. Electron.*, vol. 25, pp. 539–546, Dec. 1968.
[12] G. Gibbons and S. M. Sze, "Avalanche breakdown in read and pin diodes," *Solid-State Electron.*, vol. 11, pp. 225–235, Jan. 1968.
[13] D. L. Scharfetter and H. K. Gummel, "Large-signal analysis of a silicon Read diode oscillator," *IEEE Trans. Electron Devices*, vol. ED-16, pp. 64–77, Jan. 1969.